JFE TECHNICAL REPORT
No. 27 (Mar. 2022)

Heat Resistant Ferritic Stainless Steels (JFE-MH1, JFE-TF1™) with Super Formability to Meet CO_2 Reduction

MIYAZAKI Atsushi

Abstract:

CO_2 reduction is being vigorously promoted in each country. Reducing CO_2 emissions from internal combustion engines (including HEVs and PHEVs) is just as important as the development of BEVs and FCVs. Engine development aimed at improving fuel efficiency (CO_2 reduction) is being energetically promoted, and the demand for heat-resistant stainless steel is becoming stricter year by year. JFE Steel has contributed to the development of an excellent gasoline engine that can reduce CO_2 emissions through the development and application of heat-resistant ferritic stainless steels with super formability that pays attention to economic rationality. In this paper, metallurgical mechanism regarding improvement of heat resistance and the characteristics of the developed steels (JFE-MH1, JFE-TF1™) are reported.

1. Introduction

Plans to reduce the greenhouse gas CO_2 are being vigorously promoted in each country[1], as CO_2 is considered to be a main cause of climate change, and among those moves, electric vehicles (EV), and particularly BEV (battery EV), are now a focus of attention. If CO_2 emissions by BEV are limited to vehicle travel, that is, Tank to Wheel (TtW) emissions, the environmental performance of BEV is overwhelmingly superior to that of internal combustion engine (ICE) vehicles. However, in terms of Well to Wheel (WtW) CO_2 emissions, which also consider the CO_2 emissions from power plants that provide the electricity for batteries, the emissions from hybrids (HEV) are smaller than those from BEV in some countries[2]. Moreover, many recent reports[3–5] have compared these various types of vehicles from the viewpoint of Life Cycle Assessment (LCA), which takes into account the CO_2 emissions in the battery and power train manufacturing processes as well as scrapping and recycling vehicles. Those studies have shown that the relative superiority of gasoline and diesel vehicles, HEV and BEV varies depending on the region, travel distance and other factors because the thermal efficiency of ICE, the thermal efficiency of coal-fired thermal power plants, and the shares of renewable energy and nuclear power in the mix of electric power sources have an extremely large influence on vehicle CO_2 emissions. Based on the premise that CO_2-free energy will become the main electric power source, the countries across the world are promoting a concept that assumes a transition from ICE to HV and PHEV (plug-in hybrid vehicles) and then BEV, with BEV or FCV (fuel cell vehicles) becoming the main stream further into the future. However, based on the global composition of power sources and supply amounts at present and in the near-term future, the importance of reducing the CO_2 emissions from ICE, including emissions from internal combustion engines used in HEV and PHEV, goes without saying[3–6]. Against this background, reduction of CO_2 emissions from ICE, in other words, the development of engines with improved fuel economy, is also being promoted in parallel with the development of BEV and FCV. Focusing on domestic efforts in Japan, AICE (Research Association of Automotive Internal Combustion Engines)[6], which is a collaborative industry-academic-government initiative, set a target of 2019 for reducing the CO_2 emissions from ICE to the same level as BEV on a WtW basis, premised on a fusion of the internal combustion engine and vehicle electrification. More recently, the development of electrofuel[5] (e-fuel; fuels for gasoline and diesel vehicles produced by synthesizing CO_2 and hydrogen), which can achieve carbon neutrality while

† Originally published in *JFE GIHO* No. 48 (Aug. 2021), p. 26−33

Staff Deputy General Manager,
Stainless Steel Business Planning Dept.,
JFE Steel

utilizing existing infrastructure and engines, and dramatic improvement for the driving range of hydrogen combustion engine vehicles, which are already in practical use, by establishing a mass-production technology for high pressure hydrogen cylinders are also now attracting renewed interest.

As described above, even at present, the need for development of ICE is still large, and all auto makers are engaged in numerous research and development efforts in areas ranging from combustion technology to exhaust gas purification technology, in order to meet the environmental regulations of countries around the world. Accompanying the development of new technologies, there have also been large changes in the property requirements for materials for heat resistant engine components, particularly the exhaust manifold and catalytic converter.

JFE Steel has been contributing to the development of excellent gasoline engines that can reduce CO_2 emissions through the development of heat resistant ferritic stainless steels with super formability which also consider economic rationality[7–11], together with technologies for their application[12].

This report describes the metallurgical mechanism of improvement of the heat resistance of the material, the development guidelines for satisfying the two requirements of high formability and heat resistance, and the characteristics of the developed materials, JFE-MH1and JFE-TF1™.

2. History of Application of Stainless Steels to Engine Heat-Resistant Components of Gasoline Automobiles

Improvement of the exhaust gas purification rate of gasoline vehicles has been promoted from an early date from the viewpoint of protection of the atmospheric environment. Developments up to around the year 2000 have been described in detailed in reports by Togashi et al. and others[13, 14]. Exhaust gas, which contains CO, HC and NOx, is collected in the exhaust manifold and then purified by redox reaction in the catalytic converter (manifold converter or underfloor converter). Since the catalyst must reach the activation temperature for redox reaction, how to shorten the time to activation of the catalyst immediately after the engine is started, and how to reduce the thermal capacity of engine heat-resistant components, were important challenges of the times. Since higher exhaust gas temperatures are more effective for early activation of the catalyst, and this overlaps with the need for increased output by larger displacement, there was a tendency to expose engine heat-resistant components to higher temperature environments. Here, it may be noted that the voluntary upper limit of 280 horsepower as the maximum output of automobiles for the Japan's domestic market was abolished in 2004.

On the other hand, it is necessary to improve the thermal efficiency of engines in order to improve fuel economy. However, if too much energy is extracted from the high temperature exhaust gas after combustion, the temperature of the exhaust gas will decrease, resulting in deterioration of the purification performance of the catalytic converter, and this is a disadvantage for meeting ever-stricter emission regulations. To overcome this problem, the installation position of the converter was moved from under the floor to closer to the engine, and application of manifold converters expanded. This means that the stainless steel used in converters is also exposed to a higher temperature environment.

As a result of these changes, in the first half of the 2000s, the materials of many engine heat-resistant components were changed from cast products, Type 409 stainless steel or galvanized steel to general-purpose Type 429Nb (13-15Cr-1Si-Nb) stainless steel or high heat-resistant Type 444 (19Cr-2Mo-Nb).

3. Changes in Requirements for Engine Heat-Resistant Components Accompanying Development of Gasoline Engines with Excellent Environmental Performance

In recent years, when attention has been particularly focused on reduction of CO_2 emissions (improvement of fuel economy), which is linked to countermeasures against global warming, the following have been applied:

(1) In the air intake and exhaust system, application and expansion of the use of high compression technology, combustion chamber heat shielding, thermal energy recovery technologies, including use of the Atkinson cycle and Rankine cycle, and the EGR-C (exhaust gas recirculation cooler) to improve pumping loss caused by negative pressure.

(2) In the combustion control aspect, study of applying $\lambda<1$ control, which had been recognized as an AES (Auxiliary Emission Control Strategy), to the $\lambda=1$ region.

With the progress of these technologies[15], the environmental temperature of engine heat-resistant components has also changed greatly.

In addition, an engine with the merits of both gasoline and diesel engines have also been developed (**Photo 1** [16]). This engine achieves an extremely high compression ratio and utilizes spark controlled compression ignition (SPCCI), depending on the driving condition. This technology is considered to be one step

before homogenous charged compression ignition (HCCI), which is said to be the ultimate gasoline combustion method. This engine was a double award winner, receiving both the 60th Anniversary Memorial Prize of the Japan Stainless Steel Association (JSSA), and the 18th JSSA Award for Excellent Products, which are selected by experts in Japan's stainless steel industry[16]. In this engine, high heat resistance ferritic stainless steel with high formability was used in the heat-resistant components. Although practical application of electrically-heated catalyst systems has been extremely limited due to concerns about power shortages, this type of system was adopted independently in the internal combustion engine, envisioning general use by a fusion with electrification technology. The addition of this kind of technology has resulted in dramatic progress in reducing the CO_2 emissions of internal combustion engines, including those of HV and PHEV. On the other hand, a higher silence property has also been demanded in leading-edge ICE, and in some cases, covering the engine with a soundproof cover to reduce noise results in a further increase in the material temperature. Moreover, because higher compression ratios are impossible in gasoline engines if the residual exhaust gas is not completely discharged[17], severe shape requirements are frequently applied to the exhaust manifold, considering the smooth discharge from all cylinders.

Although the above is an example of a gasoline engine, cutting-edge CO_2 emission reduction technologies for automotive internal combustion engines, also including diesel engines, have an extremely large influence on the heat resistance and formability required in engine heat-resistant components. As a result, in addition to the need for improved heat resistance in the base material itself, improved formability has also become particularly important.

The following chapters report technologies for improving heat resistance and formability.

Photo. 1 Appearance of stainless steel exhaust manifold & converter for SKYACTIV-X engines with the world's first spark controlled compression ignition (SPCCI) (Photo courtesy: JAPAN STAINLESS STEEL ASSOCIATION)

4. Heat Resistance Improvement Technologies

4.1 High Cycle Fatigue Property at High Temperatures

In engine heat-resistant components, loading by vibrational stress caused by engine vibration occurs under a high temperature environment. As an evaluation of the high cycle fatigue property of steel sheets, the authors evaluated various types of stainless steel using a general Schenk type high cycle fatigue tester at high temperatures.

Figure 1 shows the S-N curves at 800°C of representative heat-resistant stainless steels (1.5 mmt) produced by JFE Steel. **Table 1** shows the mechanical properties of these steels at room temperature and 800°C. Although the fatigue stress at 10^7 cycles (10^7 fatigue stress) should become stress in the elastic strain range, the 10^7 fatigue stress at 800°C exceeds the tensile strength TS (JIS compliant) of the material because the strength of materials depends on the strain rate. Therefore, a simulated evaluation of the dynamic S-S curve was carried out under the same strain rate as in the fatigue test, and as a result, it became clear that 10^7 fatigue stress is within the elastic limit under this strain rate[18].

The temperature dependency of 10^7 fatigue stress is shown in **Fig. 2**. For example, the 10^7 fatigue stress of JFE409L at 700°C is equivalent to that of JFE429EX (Type 429Nb) at 780°C, and the 10^7 fatigue stress of JFE429EX (Type 429Nb) at 800°C is equivalent to that of JFE-MH1 and JFE434LN2 (Type 444) at 900°C. Since the 10^7 fatigue stress at a high strain rate, such as that in the high cycle fatigue test, is greatly affected by the strain rate as mentioned above, Fig. 1 and Fig. 2

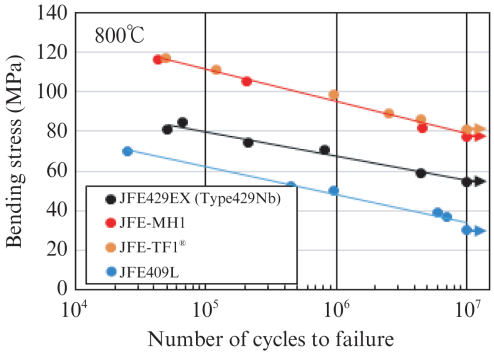

Fig. 1 Examples of S-N curve at 800°C of stainless steels

Table 1 Examples of chemical compositions and mechanical properties of heat-resistant stainless steels (2 mm t)

(mass%)

	C	Si	Cr	Nb	Mo	Cu	Al
JFE429EX (Type429Nb)	0.008	0.86	14.6	0.44	—	—	—
JFE-MH1	0.004	0.34	14.8	0.52	1.58	—	—
JFE434LN2 (Type444)	0.005	0.29	18.9	0.36	1.84	—	—
JFE-TF1®	0.007	0.80	17.5	0.45	—	1.25	added

	R.T				800°C	
	0.2%PS (MPa)	TS (MPa)	El (%)	*r*-value	0.2%PS (MPa)	TS (MPa)
JFE429EX (Type429Nb)	290	470	36	1.4	29	48
JFE-MH1	310	480	36	1.4	41	67
JFE434LN2 (Type444)	365	525	33	1.2	38	66
JFE-TF1®	400	530	33	1.4	44	63

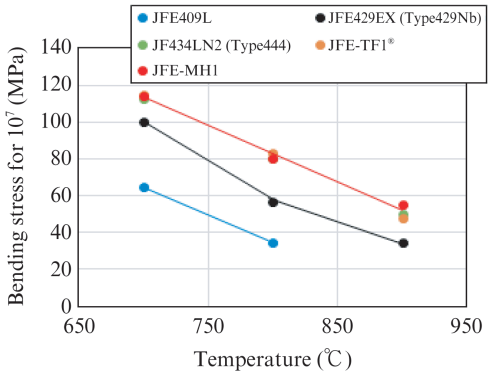

Fig. 2 Relationship between bending stress for 10^7 and temperature

are used as a relative comparison between materials.

4.2 Low Cycle Fatigue Property

In evaluations of the low cycle fatigue property of heat-resistant materials, an evaluation method in which plastic strain is loaded under a constant temperature is generally used. However, the environment temperature in automobile engines differs greatly during even a single day depending on whether the engine is running or not. Because the two ends of engine heat-resistant components are welded to other parts or joined via flanges, this is not an environment which allows free thermal expansion. Distortion by heating occurs by way of that restraint, and in some cases, low cycle fatigue caused by temperature changes is the limiting factor for the life of the parts[13, 19]. Even assuming design is conducted so as to minimize the restraint ratio as much as possible, completely eliminating plastic strain is realistically impossible. Therefore, in order to simulate the restraint environment of engine heat-resistant components, the relationship between the restraint ratio and low cycle fatigue life is evaluated by using a strain-controlled thermomechanical fatigue tester in many cases[18, 20–23].

The results of the thermomechanical fatigue test with thermal loading between 100°C and 800°C are shown in **Fig. 3**. Although the reason will be explained later, JFE-MH1 displayed the longest life at all restraint ratios. The definition of "life" used here is the widely-used criterion of the cycle in which steady stress becomes 70%. JFE409L showed longer life than that of JFE434LN2 under high restraint ratios, but when the restraint ratio was decreased, the life extension of JFE409L was slight. However, because the life of JFE434LN2 (Type 444) increased greatly at the lower restraint ratio, the order with JFE409L was reversed, and JFE434LN2 displayed the longer life. As has been pointed out by Landgraf [24], it is also possible to explain this result by the effects of strength and ductility[14, 22, 23]. In the low cycle fatigue test, the amount of plastic strain has a large effect on life. Because the amount of plastic strain is greatly affected by the strength of the material at each temperature even under the same thermal fatigue test conditions, and assuming that the coefficient of thermal expansion of the materials is the same or not different enough to cause a change in the restraint ratio, the difference in the amount of plastic strain as part of total strain depending on the material is slight in environments with large total strain (high restraint ratio). Conversely, as the total strain in an environment decreases (i.e., the restraint ratio decreases), the life of high strength materials is greatly extended because plastic strain easily becomes remarkably smaller[14]. This is self-evident from the S-S curves at each temperature. Moreover, if high temperature buckling[19] and high cycle fatigue characteristics are also considered, it can be said that aiming at the development of stainless steels with increased high temperature strength, first of all in

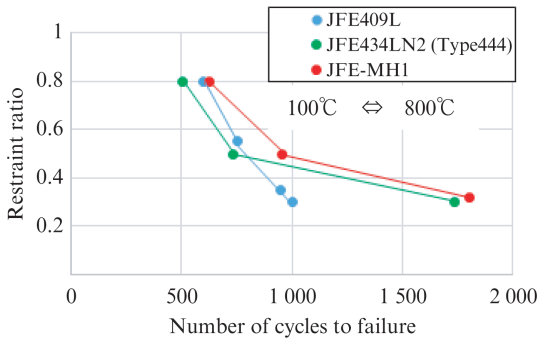

Fig. 3 Relationship between restraint ratio and number of cycles to failure in thermal fatigue test

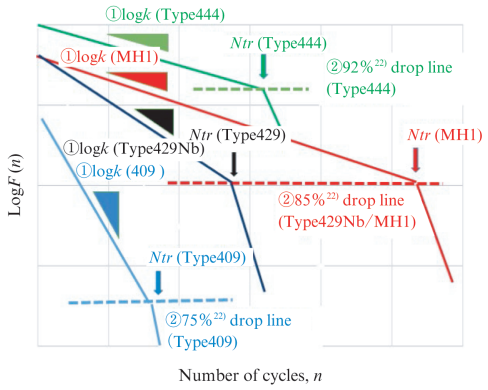

Fig. 4 Schematic diagram of effects of strength and ductility on *Ntr* (Stage I) which is considered to be cycle in which cracks occurred
$\log(F(n) = n \cdot \log(k) + \log\{\sigma(n) \cdot S(0)\}$
$(1 \leqq n \leqq Ntr \quad \sigma(n)S(0) = \text{Const.})$

order to extend thermal fatigue life, is a natural tendency.

On the other hand, in thermal fatigue testing with loading of plastic strain, plastic deformation is observed in the vicinity of the test piece fracture surface, and in many cases, plastic deformation is also observed in parts after an actual durability test. Depending on the conditions of the thermal fatigue test, the strain accumulated in the interior is recovered or relaxed at high temperatures, but nevertheless, a certain amount of plastic strain is added in each heat cycle. Because changes occur in the cross-sectional area of test pieces, the author thinks that those changes in the cross-sectional area should be considered in evaluations of the thermal fatigue property. Moreover, since changes in the cross-sectional area are also reflected in the load at the lowest temperature, the author considered the relationship between the change in the cross-sectional area and load in thermal cycling in detail, and presented a detailed description in the literature[22]. For example, let us assume hypothetically that

$$F(n) = \sigma(n) \cdot S(n) = \sigma(n) \cdot k^n \cdot S(0) \quad \cdots\cdots\cdots\cdots (1)$$

where, n: cycle number, $F(n)$: tensile load at the lowest temperature in cycle n, k: cross-sectional change ratio due to plastic deformation in 1 cycle ($0<k<1$), $\sigma(n)$: stress at the lowest temperature in cycle n and $S(n)$: cross-sectional area in cycle n.
On this assumption,

$$\log F(n) = n\log k + \log\{\sigma(n) \cdot S(0)\} \quad \cdots\cdots\cdots\cdots\cdots (2)$$

In other words, if the semilogarithmic plot $\log F(n)$-n is prepared, a straight line with a slope of $\log k$ should be obtained provided that $\sigma(n)$ and k are constant and independent of n. Type 409, Type 429Nb and Type 444 all show linearity until a specific cycle (defined as *Ntr*), which depends on the steel grade[22] (this linear condition is defined as Stage I). The order of the absolute value of the slope of $\log k$ is Type 409 > Type 429Nb > Type 444, which is the order predicted from the strength of the materials[22]. **Figure 4** shows a schematic diagram of the effect of strength and ductility on *Ntr* (Stage I). Until a certain cycle (i.e., *Ntr*), $\sigma(n)$ and $\log k$ are either constant or do not change significantly, and uniform plastic deformation (change of cross-sectional area k) continues, determined by the strength of the material and the restraint ratio, but after *Ntr*, $F(n)$ decreases sharply (defined as Stage II). In explaining this change, it is natural to think that $\sigma(n)$ decreases suddenly due to the occurrence of cracking or necking of a degree sufficient to affect $\sigma(n)$. Therefore, based on the assumption that the cross-sectional area at the time of this *Ntr* cycle represents the ductility limit of the material in that heat cycle, the author actually measured and examined the cross-sectional area[22]. If this hypothesis is correct, and also assuming a range in which the difference in the effects of solid solution and precipitation between thermal fatigue test periods is slight, the cross-sectional area ratio of the sample in the initial cycle of Stage II (*Ntr*: the cycle in which macroscopic cracking or necking of an observable degree occurs) is given as $S(Ntr) / S(0) = k^{Ntr}$ from Eq. (1), and the characteristic value of the material can be predicted independent of the restraint ratio. As the result of an experiment with a wide range of restraint ratios from 0.3 to 0.9, it was found that the k^{Ntr} of Type 409, Type 429Nb and Type 444 show material characteristic values of 0.75, 0.85 and 0.92, respectively, if the median value is taken (although with some variations attributable to the analysis), and the differences in the limits for the occurrence of cracking and necking between materials were clear, which supports the above-mentioned hypothesis[22]. From the k^{Ntr} values of the respective steels, it can be understood that the normal thermal fatigue life evaluation (i.e., $F(n)$, cycle in

which strength decreases to 70%) is the stage of Stage II (after the occurrence or cracking and necking). Thus, the k^{Ntr} value of various steels can provide a quantitative index of the relative superiority or inferiority of the materials until cracking occurs. For example, in the development of Modified 444, which has strength equal to Type 444 in the mid- to high-temperature range and ductility comparable to Type 429Nb, cracking and necking of Type 444 occurs at an integrated (cumulative) plastic deformation of around 8%, but cracking and necking are not expected to occur in the Modified 444 until cumulative plastic deformation of 15%. In other words, the life expectancy ratio until cracking is Type 444 : Modified 444 = $|\log 0.92|$: $|\log 0.85| \fallingdotseq 1 : 1.9$, meaning that the cracking and necking life of Modified 444 is extended by nearly 2 times, regardless of the restraint ratio.

In environments in which only heat cycle loading is applied, there is little meaning in discussing *Ntr* (separation of Stage I and Stage II), which was defined as the cycle at which cracking and necking occurs. However, in the case of actual engine heat-resistant components, which are also subjected to loading by mechanical vibration, as described in sections 4.1 and 4.3, there are also cases where the occurrence of cracking and necking due to thermal cycling substantially shortens the high cycle fatigue life determined by mechanical vibration. That is to say, there is possibility of the life of the component may be shortened composite fatigue consisting of thermal cycling (low cycle fatigue) + mechanical vibration (high cycle fatigue), and in this case, *Ntr*, defined as the cycle at which cracking and necking occurs, has an extremely important meaning, depending on the magnitude of the vibration in high cycle fatigue. Although the thinking on the life of the target components is case-by-case, it is rational to assume, for example, that thermal fatigue life is determined by the cycle in which stress drops to 75% for Type 409, 85% for Type 429Nb and 92% for Type 444, and not the cycle in which stress drops to a uniform 70% regardless of the steel grade. Therefore, based on the schematic diagram in Fig. 4, the basic thinking on increasing material life is that the following (1) and (2) are effective.

(1) Reduction of plastic deformation by higher strength in the mid- to high-temperature region (slope $\log k \rightarrow 0$)
(2) Increase limit ductility (particularly effective if (1) is on the same level)

The point that higher strength is effective for reducing the amount of plastic deformation, that is, for achieving $\log k$ that approaches $\log k \rightarrow 0$, was discussed in Section 4.2. However, the fact that higher strength is generally associated with a decrease in limit ductility is clear from the comparison of the k^{Ntr} of Type 409, Type 429Nb and Type 444 (0.75, 0.85, 0.92, respectively). Accordingly, higher strength results in an earlier cracking and necking cycle (*Ntr*) and is not an advisable strategy.

That is, when attempting to achieve high ductility, in addition to whether forming is possible or not, extension of the components life until cracking and necking occurs due to thermal fatigue (i.e., Stage I life) is also very important. Moreover, since this ductility effect does not depend on the restraint ratio, assuming $\log k$ is the same, a life extension effect corresponding to the ratio of k^{Ntr} can be expected, even under a low restraint ratio, which is normally considered to be the region where strength is the controlling factor.

Based on this viewpoint[22], the authors developed JFE-MH1[9, 10], which is based on a low alloy composition design ductility while also maintaining the mid- to high-temperature strength of Type 444.

4.3 Composite Fatigue

If sheet thickness reduction due to plastic deformation proceeds in a low cycle fatigue environment, such as thermal fatigue, the stress caused by external vibration will increase in that area. Therefore, even if a part fails in a durability test and striations (traces of high cycle fatigue) are observed on the fracture surface, it would be hasty to attribute the cause of failure to high cycle fatigue simply because striations were detected. In other words, the possibility that the root cause of high cycle fatigue failure was plastic deformation or cracking and necking caused by low cycle fatigue should also be considered.

If it can be concluded that the true cause is reduction of sheet thickness or cracking and necking caused by low cycle fatigue due to thermal cycling, one effective option is to modify the shape or the material so as to actively change the temperature distribution, rather than increasing the sheet thickness, which has only a limited effect. In investigations of the cause of damage in durability tests, in many cases the cause can only be clarified by making the maximum possible use of knowledge and information including materials science, metallurgical engineering, forming/heat simulation, high/low cycle fatigue theory, oxidation, corrosion, etc.

5. Heat Resistance Improvement Technology by Formability Improvement

5.1 Background of High Formability

Sections 4.2 and 4.3 pointed out that high ductility has an important meaning for the low cycle fatigue property regardless of the magnitude of the restraint

ratio.

Type 444 is generally considered to be highest heat-resistant SUS among ferritic stainless steels available in the market. However, if high temperature strength is increased by adopting a high alloy approach, ductility will be reduced over the entire temperature range, from room temperature to high temperatures, because strength will also be increased at other temperatures[22]. Heat resistance is normally evaluated in terms of fatigue, oxidation resistance, high temperature strength or other properties using a sheet or round bar test piece, in other words, with the material in the unformed condition. However, as described in Chapter 3, engine heat-resistant components are frequently subjected to severe forming. There are many reasons for this, such as engine performance, limitations on engine space, and the like. The sheet thickness is reduced by this kind of severe forming, and if this occurs locally, necking will occur and application is impossible. Moreover, even if necking does not occur, if the reduction of sheet thickness is large, it will be necessary to increase the thickness, including parts where this is not inherently needed, and this will lead to increased vehicle weight and reduced fuel economy. JFE Steel is conducting research which considers higher formability, assuming cases where this kind of severe forming is demanded.

5.2 Technology for Improvement of Lankford Value (*r*-Value)[8]

It is known that the Lankford value (hereinafter, *r*-value) of ferritic stainless steels changes greatly depending on the manufacturing process. Although the *r*-value is improved by applying a high cold-rolling reduction ratio of 70% or more[25], an adequate cold-rolling reduction ratio cannot be secured with the stainless steels applied in engine heat-resistant components because the material thickness is only 1.5 mm to 2.5 mm. Even under this restriction, JFE Steel succeeded in improving the *r*-value without changing other properties by applying texture control. The *r*-value of JFE429EX (Type 429Nb) with a thickness of 2 mm is improved by approximately 40%, from 1 to 1.4, through the high *r*-value process. This improvement of the *r*-value not only remarkably improves the drawability and stretch-flanging ratio (hole expandability) of steel sheets, but overwhelmingly improves the formability of pipes[8].

As shown in Table 1, JFE Steel's heat-resistant ferritic stainless steels (JFE429EX (Type 429Nb), JFE-MH1 and JFE-TF1™) all have high *r*-values. In addition to the ease of molding parts, these materials also to contribute to improved durability by suppressing sheet thickness reduction.

5.3 JFE-MH1[9, 10] with Thermal Fatigue Property Superior to High Heat-Resistance Grade (JFE434LN2) while Maintaining Super Formability of General Grade (JFE429EX) Based on Multi-Role Concept

As described in Chapters 1 to 3, JFE429EX (Type 429Nb) is a general-purpose material for engine heat-resistant components. If requirements cannot be satisfied with this grade and trial use of JFE434LN2 (Type 444) is attempted, modification of the dies, process changes, etc. are frequently necessary because the room temperature yield strength (YS) and elongation (El) of the two materials differ greatly. For this reason, a steel which improves high temperature strength while maintaining room temperature formability (high *r*-value, high El, low YS) comparable to that of the high *r*-value product JFE429EX (Type 429Nb) had been strongly demanded.

Among the mechanical properties of JFE-MH1 shown in Table 1, JFE-MH1 has the same high temperature strength as JFE434LN2 (Type 444) while continuing to provide the same high room temperature formability as JFE429EX (Type 429Nb). Therefore, when the durability of JFE429EX (Type 429Nb) is inadequate, durability testing can be carried out with JFE-MH1 without changing the trial production dies, etc., which greatly contributes to speeding up engine development. The following discusses the metallurgical mechanism of JFE-MH1 with increased high temperature strength while maintaining the same room temperature formability (high *r*-value, high El, low YS) as JFE429EX (Type 429Nb), which has received a high evaluation in the market.

In the case of JFE429EX (Type 429Nb), high oxidation resistance at around 950˚C in the atmosphere is secured by a 15% Cr composition with addition of approximately 1% Si. It is generally thought that improvement of oxidation resistance by Si is an effect of a highly protective oxidation film, but that type of film is not observed when 1% Si is added to 15% Cr[10]. Fujikawa et al.[26] reported that an "Breakaway oxidation phenomenon" occurs from the sites where the ferrite microstructure undergoes the γ transformation at high temperature, and proposed that the mechanism of oxidation resistance by Si can be explained by the stability of the ferrite microstructure rather than by a protective film. According to the theory proposed by Fujikawa et al., because even Mo, which does not form a highly protective oxidation film, is a ferrite-forming element, it is conceivable that the above-mentioned breakaway oxidation at around 950˚C is suppressed through high temperature stabilization of the ferrite phase of 15% Cr stainless steel. On the other hand, it is

clear that Mo, which is a heavy element, improves high temperature strength by solid solution strengthening, even with a 15% Cr base. In other words, while Si plays only the one role of improving oxidation resistance, Mo can play the two roles of oxidation resistance and high temperature strength. Therefore, we developed a steel with added Mo, assuming that Mo is advantageous for softening at room temperature.

Figure 5 (a) and **(b)** show the effects of Mo on oxidation resistance at 950˚C in a 15% Cr-0.2% Si base steel and in a 15% Cr base steel[10]. In spite of the fact that Mo does not form a highly protective Mo oxidation film, oxidation resistance was improved remarkably by addition of 1.5% Mo or more. Moreover, in the case of the 15% Cr-1.6% Mo base, oxidation resistance at 950˚C also improved dramatically, even with addition of 0.2% or more of Si, which does not form a highly protective oxidation film. These results strongly support the ferrite phase theory[26] of Fujikawa et al. that ferritic stainless steel prevents breakaway oxidation. It may be noted that a 15Cr composition design was also adopted for JFE-MH1 based on the knowledge[7] gained in the development of JFE429EX (Type 429Nb) that solid solution strengthening at high temperature cannot be expected with Cr, which is a comparatively light element similar to Fe, and because Cr increases room temperature strength due to the difference between its atomic radius and that of Fe, causing deterioration of ductility, it is advisable to secure the necessary minimum level of Cr considering corrosion resistance, etc. Thus, JFE-MH1, which displays the target properties, was developed based on the metallurgical principle of utilizing one element (Mo) in the improvement of multiple properties[9, 10].

5.4 JFE-TF1 with Thermal Fatigue Property Superior to High Heat-Resistance Grade (JFE434LN2) while Maintaining High *r*-Value of General Grade (JFE429EX)

In JFE-TF1, as shown in Table 1, fatigue property at high temperatures and thermal fatigue property

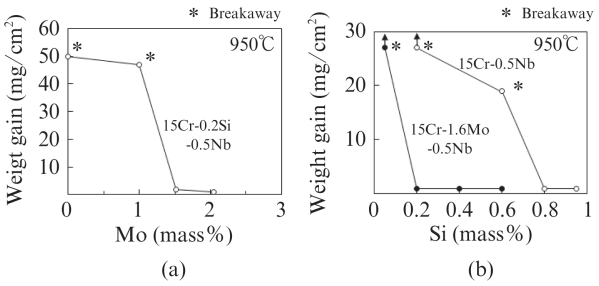

Fig. 5 Effects of (a) Mo and (b) Si contents on weight gain of 15%Cr-Nb stainless steels by continuous heating at 950˚C for 200 h in air

comparable to those of JFE-MH1 are achieved with a Mo-free composition design because precipitation strengthening by Cu addition[11, 27, 28] and solid solution strengthening by Al[11] are used. On the other hand, although its strength is higher than that of JFE434LN2 (Type 444), its *r*-value is also high. This means that JFE-TF1 can be used in many cases in parts that do not require such severe forming that JFE-MH1 is necessary.

6. Conclusion

This paper has presented an overview of the concepts and features of JFE Steel's high heat-resistant ferritic stainless steels with super formability. The positioning of the developed steels (JFE-MH1, JFE-TF1) and the existing steels (JFE429EX (Type 429Nb), JFE434LN2 (Type 444) is shown in **Fig. 6**. The developed steel JFE-MH1 has room temperature high formability (high *r*-value, high elongation (El) and low yield strength (YS)) comparable to that of JFE429EX (Type 429Nb) while continuing to maintain a thermal fatigue property superior to that of JFE434LN2 (Type 444) in the base material itself, and the developed Mo-free JFE-TF1 has a high *r*-value equal to that of JFE429EX while maintaining a thermal fatigue property equal or superior to that of JFE434LN2 (Type 444) in the material itself. In addition to expanding the formable range, this excellent formability (high *r*-value and high elongation (El)) also makes an important contribution to improving the durability of components made from those materials. Components in which the developed steels were applied have an extensive record of use, demonstrating higher durability than that of Type 444 as a result of the durability improvement mechanism outlined in Sections 4.2 to 5.2.

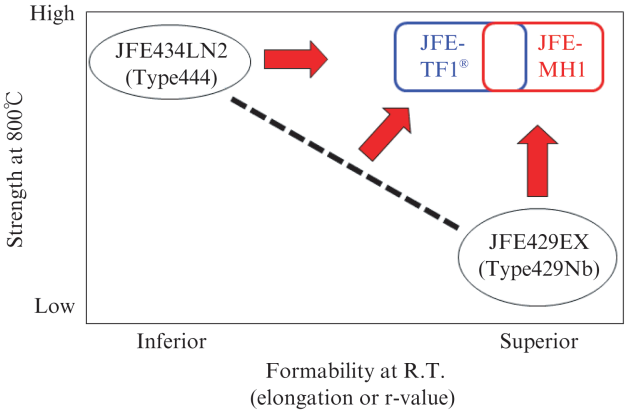

Fig. 6 Comparison of characteristics at R.T. and 800˚C between conventional (Type444 & Type429Nb) and developed stainless steel (JFE-MH1 & JFE-TF1™)

At present, many technology development efforts are in progress in industry, academia and government agencies with the aim of reducing CO_2 emissions from internal combustion engines (including those used in HV and PHEV). With the expanding needs for higher heat resistance than the general-purpose grade JFE429EX (Type 429Nb), it is expected that JEF-MH1 and JFE-TF1 will continue to make important contributions in the future as well.

References

1) For example, Prime Minister Suga's statements of belief at the 230th Diet in Japan on October 26, 2020.
2) Nikkei Automotive. Jan. 2020, p.94.
3) JAMAGAZINE. Japan Automobile Manufacturers Association. 2021, vol.55, Jan-Feb, p.11.
4) Kawamoto, R.; Mochizuki, H.; Moriguchi, Y.; Nakano, T.; Motohashi, M.; Sakai, Y.; Inaba, A. Estimation of CO_2 Emissions of Internal Combustion Engine Vehicle and Battery Electric Vehicle Using LCA. Sustainability. 2019,11, p. 2690–2704.
5) Nikkei Automotive. Feb, 2021, p4.
6) https://www.aice.or.jp/company/
7) Miyazaki, A; Gunji, M.; Yoshioka, K. Development of High Formability R429EX and Heat-Resistant R444EX Stainless Steels for Automotive Exhaust Manifold. Kawasaki Steel Giho. 1993, vol. 25, no2, p. 34–40.
8) Miyazaki, A.; Gunji, M.; Baba, Y. Ferritic Stainless Steels and Pipes for Automotive Exhaust Systems to Meet Weight Reduction and Stricter Emission Requirements. Kawasaki Steel Technical Report. 2002, no.46, p. 19–24.
9) Miyazaki, A.; Hirasawa, J.; Furukimi, O.; Kobayashi, M.; Kakihara, S. Development of High Heat-Resistant Ferritic Stainless Steel with High Formablity,"RMH-1". For Automotive Exhaust Gas Systems. Materia Japan. 2003, vol. 42, no.2, p. 157–159.
10) Miyazaki, A.; Hirasaw, J.; Furukimi, O. Ferritic Stainless Steel for Automotive Exhaust Systems —High Heat-Resistant Ferritic Stainless Steel with High Formability for Automotive Exhaust Manifolds "JFE-MH1"—. JFE Technical Report. 2004, no4, p. 61–66.
11) Nakamura, T.; Ota, Y,; Kato, Y. Development of Resource conserving Heat resistant Ferritic Stainless Steel "JFE-TF1". Materia Japan. 2015, vol. 54, no1, p. 18–20.
12) Ozaki, Y.; Iguchi, T.; Ujiro, T. Formability of the Ferritic Stainless Steel for Exhaust Manifold. JFE Giho. 2008, no. 20, p. 42–46.
13) Togashi, F. Recent Progress of Stainless Steels for Automotive Exhaust System. Nishiyama Memorial Lecture. 1994, p. 267–293.
14) Miyazaki, A.; Hirasawa, J.; Furukimi, O. Advancd Stainless Steel for Automotive Exhaust Gas System. Journal of Society of Automotive Engineers of Japan. 2001, vol. 55, no. 10, p. 25–30.
15) Nikkei Automotive. Feb. 2021, p. 38.
16) http://www.jssa.gr.jp/prize/ the 60th Anniversary Memorial Prize of the Japan Stainless Steel Association (JSSA) and the 18th (2019) JSSA Award for Excellent Products.
17) Mihori, N.; Supervised by Hitomi, M. Development of MAZDA SKYACTIV Engines. MIKI PRESS. 2016, 201p. (p. 33)
18) Miyazaki, A.; Ishii, K.; Sato, S. Ferritic Stainless Steels with Good High Temperature Fatigue and Thermal Fatigue Properties for Automobile Exhaust Gas Systems. Kawasaki Steel Giho. 1998, vol. 30, no. 2, p. 31–35.
19) Yamanaka, M.; Otoguro, Y. ; Miura, F.; Zaizen, T. Stainless Steels for high temperatures. Seitetsu Kenkyu. 1983, no. 311, p. 33–39.
20) Hirakawa, K.; Tokimasa, K. Thermal Fatigue of Ferritic Stainless Steel, 430Zr. Tetsu to Hagane. 1977, vol. 63, no.4, S255.
21) Oku, M.; Nakamura, S.; Hiramatsu, N. Thermal Fatigue and High temperature Properties of Ferritic Stainless Steels. Nisshin Steel technical report. 1992, no. 66, p. 37–48.
22) Miyazaki, A.; Tada, M.; Togashi, F. Effect of Alloying Elements on High Temperature Property of Ferritic Stainless Steels for Exhaust Manifold. Journal of Society of Automotive Engineers of Japan, Pre-Academic Lecture Printing. 1993, no. 936, p201–204.
23) Miyazaki, A.; Ishii, K.; Hirasawa, J.; Satoh, S. Fatigue Properties of Nb-Bearing Stainless Steels for High Temperature Applications in Automobile Exhaust Gas System. SAE Technical Paper. 1999–01-0373, 1999, p. 1–8.
24) R, W, Landgraf. The Resistance of Metals to Cyclic Deformation. ACHIEVEMENT OF HIGHFATIGUE RESISTANCE IN METALS AND ALLOYS, ASTM STP467, 1970, p. 3–36.
25) Sawatani, S.; Shimizu, K.; Nakayama, T.; Miyoshi, M. r-value and texture of Ti-added 17%Cr Ferritic Stainless Steel. Tetsu to Hagane. 1977, vol. 63, no. 5, p. 843–854.
26) Fujikawa, H.; Murayama, J.; Fujino, M. High Temperature Oxidation Resistance and Oxidation Mechanism of Ferritic Stainless Steels. Testu to Hagane. 1983, vol. 69, no. 6, p. 678–685.
27) Tomita, T.; Oku, M. Development of Cu Bearing Ferritic Stainless Steel, NSSEM-C. Nisshin Steel technical report. 2009, no. 90, p. 30–39.
28) Hamada, J.; Hayashi, A.;Kanno, N.; Komori, T.; Ito, K.; Fukuda, N.; Inoue, Y. Development of Heat resistant Ferritic Stainless Steels "NSSC ®429NF" and "NSSC ®448EM" Utilized Dynamic Precipitation Hardening for Automotive Exhaust Systems. Materia Japan. 2017, vol. 56, no. 1, p. 33–35.